

# RSC Advances



This is an *Accepted Manuscript*, which has been through the Royal Society of Chemistry peer review process and has been accepted for publication.

*Accepted Manuscripts* are published online shortly after acceptance, before technical editing, formatting and proof reading. Using this free service, authors can make their results available to the community, in citable form, before we publish the edited article. This *Accepted Manuscript* will be replaced by the edited, formatted and paginated article as soon as this is available.

You can find more information about *Accepted Manuscripts* in the [Information for Authors](#).

Please note that technical editing may introduce minor changes to the text and/or graphics, which may alter content. The journal's standard [Terms & Conditions](#) and the [Ethical guidelines](#) still apply. In no event shall the Royal Society of Chemistry be held responsible for any errors or omissions in this *Accepted Manuscript* or any consequences arising from the use of any information it contains.

Table of Contents (TOC) Entry

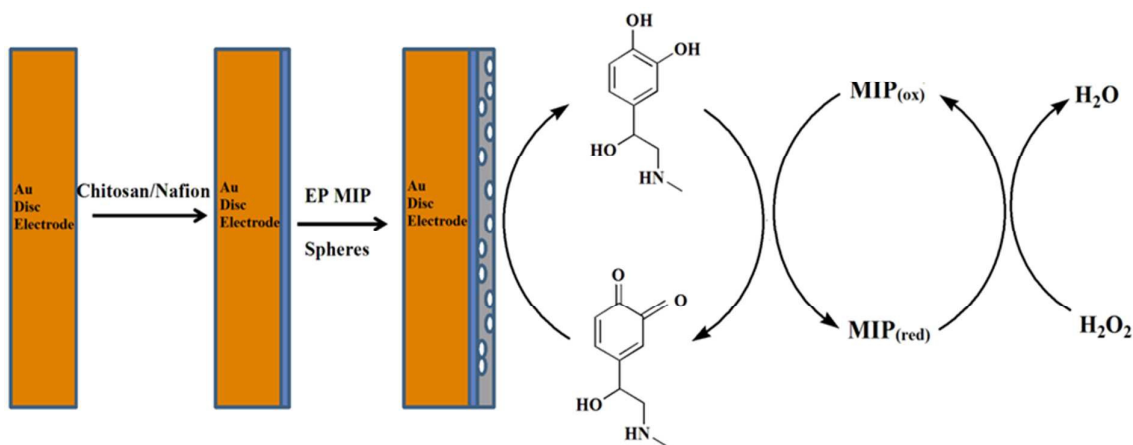
# Electrochemical Detection of Epinephrine Using a Biomimic Made Up of Hemin Modified Molecularly Imprinted Microspheres

**Kiran Kumar Tadi,<sup>a</sup> Ramani V. Motghare,<sup>a,\*</sup> V. Ganesh<sup>b,c,\*</sup>**

<sup>a</sup> *Chemistry Department, Visvesvaraya National Institute of Technology, Nagpur – 440010, India. Telephone: +91-712-2801603*

<sup>b</sup> *Electrodics and Electrocatalysis (EEC) Division, CSIR – Central Electrochemical Research Institute (CSIR – CECRI), Karaikudi – 630003, Tamilnadu, India. Telephone: +91-4565-241242. Fax: +91-4565-227779.*

<sup>c</sup> *Academy of Scientific and Innovative Research (AcSIR), New Delhi – 110025, India.*

TOC Graphics

Electrochemical detection of epinephrine, an important neurotransmitter in mammalian central nervous system is demonstrated in this work using a simple bio-mimic prepared by hemin modified microspheres of molecularly imprinted polymer.

# Electrochemical Detection of Epinephrine Using a Biomimic Made Up of Hemin Modified Molecularly Imprinted Microspheres

**Kiran Kumar Tadi,<sup>a</sup> Ramani V. Motghare,<sup>a,\*</sup> V. Ganesh<sup>b,c,\*</sup>**

<sup>a</sup> *Chemistry Department, Visvesvaraya National Institute of Technology, Nagpur – 440010, India. Telephone: +91-712-2801603*

<sup>b</sup> *Electrodics and Electrocatalysis (EEC) Division, CSIR – Central Electrochemical Research Institute (CSIR – CECRI), Karaikudi – 630003, Tamilnadu, India. Telephone: +91-4565-241242. Fax: +91-4565-227779.*

<sup>c</sup> *Academy of Scientific and Innovatibe Research (AcSIR), New Delhi – 110025, India.*

*\* To whom correspondence should be addressed*

*V. Ganesh; E-mail: [vganesh@cecri.res.in](mailto:vganesh@cecri.res.in) (or) [ganelectro@gmail.com](mailto:ganelectro@gmail.com)*

*R. V. Mothgare; E-mail: [rkkawadkar@chm.vnit.ac.in](mailto:rkkawadkar@chm.vnit.ac.in)*

## Abstract

In this work, a highly sensitive and selective molecularly imprinted polymer (MIP) is synthesized using a functional monomer, 2,4,6-trisacrylamido-1,3,5-triazine and demonstrated its application for electrochemical detection of epinephrine (EP). This particular monomer is selected based on the interaction energies computed for the formation of pre-polymer complex using computational studies. Further EP imprinted microspheres are prepared by precipitation polymerization using hemin as the catalytic centre in order to mimic the active site of enzyme like peroxidase. Molecularly imprinted and non-imprinted microspheres are characterized by using fourier transform infrared spectroscopy (FTIR) and field emission scanning electron microscopy (FESEM). Electrochemical sensor for EP detection is fabricated by modifying a gold disc electrode with molecular imprinted microspheres stabilized by chitosan/nafion mixture. A linear concentration range of  $5 \times 10^{-8}$  M to  $40 \times 10^{-6}$  M with a very low detection limit of  $1.2 \times 10^{-8}$  M (S/N = 3) is determined for the proposed sensor. Our results clearly demonstrate an efficient sensing capability of imprinted polymer with good reproducibility, stability and higher selectivity for EP detection over its other structural analogues and potential interferants. Essentially the proposed electrochemical sensor follows a cascade reaction mechanism since it consists of two catalytic sites that aid in EP detection. Analytical applicability of this sensor towards the determination of EP is demonstrated using human blood serum and injection samples.

**Keywords:** *Electrochemical biosensor; Epinephrine; Molecularly imprinted polymers; Microspheres; Gold disc electrode; Computational studies.*

## 1. Introduction

Epinephrine (4-[(1R)-1-hydroxy-2-(methylamino)ethyl]benzene-1,2-diol) [EP] is an important neurotransmitter in mammalian central nervous system and acts as a chemical mediator for transferring the nerve impulses to different organs; thereby controlling its performance in biological reactions and nervous chemical processes.<sup>1</sup> Many diseases like contraction of smooth muscles, blood pressure, glycogenolysis in the liver and muscle, and lipolysis in adipose tissue are related to changes in concentration of EP in the living mammalian system. EP has also been used as a common emergency healthcare medicine.<sup>2</sup> Enzyme mimics that possess the structure and activity close to that of natural enzymes can be prepared by molecular imprinting technique.<sup>3</sup> Generally, this technique involves the creation of selective recognition sites in synthetic polymers and the principle is similar to that of enzyme specificity proposed by Fischer as early as 1894.<sup>4</sup> Preparation of molecularly imprinted polymers (MIPs) involves the formation of self-assembly between a functional monomer and the analyte (template), followed by co-polymerization of cross linker via either thermal or UV radiation. Extraction of pre-formed template leads to the formation of cavities or patterns that are complementary to the shape and size of the template present within the polymer matrix.<sup>5</sup> In the last two decades, MIPs became increasingly attractive in many fields of chemistry and biology due to their versatile applications and catalytic properties, particularly for sensor applications.<sup>6-8</sup> These new kind of enzyme mimics have a lot of advantages such as moderate cost, ease of preparation and long time stability compared to the traditional mimics of natural antibodies and enzymes.<sup>9</sup>

Although synthesis of MIPs seems quite easy, screening of the best functional monomer having more binding interactions with the selective template makes the imprinting, a tedious and

time consuming technique.<sup>10</sup> Combinatorial chemistry and molecular modeling are the two most promising tools for the identification of a suitable monomer to the development of MIPs with enhanced recognition properties.<sup>11</sup> In general combinatorial methods are more rapid than the traditional approaches,<sup>12</sup> but they are expensive as many conditions are required for necessary evaluation and identification. Combinatorial screening is not just a predictive tool but involves a laborious experimental verification procedures.<sup>13</sup> Computer aided study of MIPs is a rational and fast method to improve their recognition properties. *Ab initio* calculations based on quantum mechanics at different levels, such as Hartree–Fock,<sup>14</sup> Moller Plesset<sup>15</sup> or density functional theory (DFT)<sup>16</sup> have been employed to rationally design the desired MIPs. Among the various methods, DFT provides a high level accuracy information with reasonable and affordable computational costs.<sup>17</sup>

Several methods have been developed till date to determine EP in pharmaceutical and clinical samples. Conventional methods namely high performance liquid chromatography (HPLC),<sup>18</sup> chemiluminescence,<sup>19</sup> fluorimetry,<sup>20</sup> spectrophotometry,<sup>21</sup> capillary electrophoresis<sup>22</sup> and flow injection analysis<sup>23</sup> have been reported. Recently, electroanalytical techniques became popular for the determination of environmental and biological compounds due to their ease of detection, sensitivity, stability, accuracy, lower cost and simplicity etc.<sup>24–26</sup> Electrochemical detection of EP on bare surfaces (unmodified electrodes) has some fundamental problems, mainly arising from high overpotential associated with the detection of analyte and sluggishness of the electrode kinetics. Various strategies including electrochemically pretreated glassy carbon electrode (GCE),<sup>27</sup> polymer modified GCE and self-assembled monolayer modified Au electrodes<sup>28,29</sup> are used for the analysis.

Keeping this in mind, in the present work, an electrochemical detection of EP is demonstrated using hemin modified microspheres of MIP. A functional monomer namely 2,4,6-trisacrylamido-1,3,5-triazine (TAT) derived from triamino triazine, is used for the preparation of EP imprinted polymer and this is been selected based on the computational studies. This particular MIP has a compact, symmetric and rigid structure (supporting information; Fig. S1) that can facilitate multiple non-bonding interactions in the well defined three dimensional preferences.<sup>30</sup> Preparation of MIP using precipitation polymerization method involves the use of TAT as a functional monomer and chlorohemin as a co-monomer having catalytic activity for specific recognition of the template and replacing the natural enzyme chloroperoxidase.<sup>31,32</sup> Chlorohemin is covalently linked to the polymer during polymerization and incorporation of chlorohemin leads to the formation of active sites into MIP that is further utilized for the catalytic reduction of hydrogen peroxide ( $\text{H}_2\text{O}_2$ ). Hemin in the MIPs can be oxidized by  $\text{H}_2\text{O}_2$  and then re-reduced by EP. The later reaction involves the formation of EP-quinone, which is electroactive and can be reduced further, leading to an overall cascade reaction for the determination of EP. MIP is immobilized on Au electrode surface along with chitosan due to its effective transduction, membrane forming ability, biocompatibility and detection in aqueous system with a longer period stability.<sup>33</sup> After MIP immobilization, a thin layer of Nafion is coated over the surface to stabilize MIP because of its chemical and mechanical stability, along with the cationic selectivity and higher conductivity.<sup>34</sup> Differential pulse voltammogram (DPV) assays are performed for the detection and quantification of EP in the present work. The creation of binding sites in EP MIP provides a better enhancement in sensitivity of the proposed sensor. Various important parameters such as the amount of MIP to be coated, concentration of  $\text{H}_2\text{O}_2$  and pH of the electrolytic medium which influences the sensitivity and selectivity of the

electrochemical sensor are optimized. The fabricated electrochemical biosensor showed excellent performance characteristics for the determination of EP. Further the feasibility of the proposed sensor for detecting EP in human blood serum and injection samples is demonstrated for practical applications.

## 2. Experimental Section

### 2.1. Chemicals

Epinephrine (EP), melamine (Mel), 2,2'-azoisobutyronitrile (AIBN) and ferri protoporphyrin IX (hemin) were purchased from Sigma–Aldrich. Ethylene glycol dimethacrylate (EGDMA), acryloyl chloride (AC) and acetonitrile (HPLC grade) were obtained from Merck chemicals. Similarly (-)-Isoproterenol hydrochloride (IP), 3,4-dihydroxy-L-phenylamine (HPA), 3,4-dihydroxyhydrocinnamic acid (HCA), L-ascorbic acid (LAA) and 1,2-dihydroxy naphthalene (DN) were procured from Sigma–Aldrich. All these chemicals were of analytical grade and used as such without any further purification. All the aqueous solutions were prepared using Millipore water having a resistivity of 18.2 MΩ cm obtained from Milli–Q system (Millipore Inc.).

### 2.2. Hardware and software

A personal computer namely Intel Pentium 4 running with Red Hat Linux operating system, 2.0 GHz CPU, 2 GB RAM having 200 GB hard disc was used for the computational studies involving simulation of functional monomers. This system was used to execute software package Gaussian 03. Avogadro 1.0.1 was employed as a graphical user interface for Gaussian.

### 2.3. Geometry optimization and energy calculations

Three-dimensional structures of the template, monomer and monomer–template complexes were built with the aid of Avogadro program. The virtual library of functional monomers essentially consists of acidic, basic and neutral monomers. The molecular geometries were optimized by using DFT calculations at the B3LYP/6-31G(d) level implemented in Gaussian 03 and the single point energies were calculated by B3LYP/6-31+G(d,p) level of theory.<sup>35</sup> The interaction energy ( $\Delta E$ ) values of pre-polymerization complexes were calculated by using eq. 1 given below.

$$\Delta E = E_{(\text{template-monomer})} - E_{\text{template}} - \sum E_{\text{monomer}} \quad (1)$$

where  $E_{(\text{template-monomer})}$  is the energy of template–monomer complex,  $E_{(\text{template})}$  is the energy of EP and  $E_{(\text{monomer})}$  is the energy associated with a functional monomer. Basis set superposition error (BSSE) which often substantially affects the calculated stabilization energy values, was corrected by means of the counterpoise method.<sup>36</sup>

### 2.4. Synthesis of functional monomer

The selected functional monomer, TAT was synthesized using a procedure reported elsewhere.<sup>30</sup> Melamine (Mel) (20 mmol) was dissolved in 20 mL of dimethyl formamide (DMF). AC (65 mmol) was gradually added to Mel in DMF and the reaction mixture was stirred for about 10 hours. Then the resultant mixture was washed with hot (35°C) DMF–water (10 mL; 1:1 v/v) to remove the residual precursors. The product obtained was then characterized by FTIR, <sup>1</sup>H NMR, and elemental analysis: CHN analysis (Found: C–49%; H–4.5%; N–30.1% and the formula C<sub>12</sub>H<sub>12</sub>N<sub>6</sub>O<sub>3</sub> requires C–49.9%; H–4.1%; N–29.3%). <sup>1</sup>H NMR,  $\delta$  ppm d<sub>6</sub> DMSO, 7.75 (s, 1H, –NH), 3.45 (s, 1H, –CH) and 2.50 (s, 1H, –CH<sub>2</sub>). FTIR (KBr), cm<sup>-1</sup>: 1681 (amide I),

1487 (amide II), 3329 (–NH stretching; broad), 3118 (CH stretching), 1338 (–C–N– stretching), 1004 (–CH bending) and 772 (–CH<sub>2</sub> rocking vibration of alkene). These studies clearly reveal the successful synthesis of functional monomer, TAT.

## 2.5. Preparation of EP imprinted and non-imprinted microspheres

Hemin modified EP imprinted polymer (MIP) was prepared using non-covalent immobilization protocol (supporting information; Fig. S2). Accordingly, the pre-polymerization complex was prepared by mixing 0.5 mmol EP (template), 2 mmol TAT (functional monomer) and 5 mL mixture of DMSO and acetonitrile (3:2 v/v), in 15 mL glass vial. The contents were shaken well to allow the formation of self-assembly by host–guest chemistry. Subsequently, 5 mmol EGDMA (cross linker), 0.02 mmol hemin and 0.1 g AIBN were sequentially added. The mixture was then sonicated and purged with nitrogen gas for 10 minutes to create an inert atmosphere. The vial was completely sealed and kept in a water bath at 60°C for 15 hours to complete the polymerization reaction. Then the polymer was washed with excess of methanol to remove any residual precursors. The resultant polymer was observed to be microspheres and were collected on a nylon filter (0.27 µm pore size); washed repeatedly with methanol – acetic acid (9:1 v/v) mixture to remove the template. The reference or non-imprinted polymer (NIP) was also prepared in same manner, following the above mentioned procedure but in the absence of template, EP.

## 2.6. Preparation of MIP modified electrode

Initially bare gold disc electrode was cleaned by polishing with alumina slurry and ultrasonically cleaned with de-ionized water, absolute ethanol and millipore water each for 5

minutes respectively. Then the electrode was cleaned with a hot mixture of “*piranha*” solution (1:3 mixture of 30% H<sub>2</sub>O<sub>2</sub> and conc. sulphuric acid), rinsed with ultra-pure water and dried. Followed by polishing, the electrode was subjected to a potential cyclic sweeping between -0.4 V and 1.6 V in 0.5 M H<sub>2</sub>SO<sub>4</sub> until a constant cyclic voltammogram representing the electrochemical characteristics of a bare gold electrode (gold oxide formation and stripping peaks) was obtained. Initially, 5 μL of 1% chitosan in 0.8% acetic acid was coated onto the pre-cleaned gold disc electrode and dried for an hour. About 1 mg of EP imprinted microspheres dispersed in 1 mL of 0.1 M phosphate buffer solution (PBS) (pH=7.0) were sonicated for 10 minutes. 10 μL of this well dispersed MIP (1 mg/mL) in PBS (pH=7.0) solution was drop casted onto the chitosan modified Au disc electrode and dried in air. Finally, 5 μL of 0.5% Nafion in acetonitrile solution was coated onto the electrode to obtain chitosan/MIP/Nafion modified Au surface and this electrode was explored further for the detection of EP. This modified electrode was stored at 4°C when not in use. Analytical applicability of the proposed sensor was investigated for EP detection using human blood serum samples and injection solutions as model systems. EP hydrochloride injection samples were purchased from a local pharmacy with proper approval and permission. Human blood serum samples were obtained from a local pathology clinic with a proper permission. All these experiments were performed in compliance with the relevant laws and institutional guidelines and the institutional committees have approved these experiments. It is also worth mentioning here that informed consent was obtained for these experimentations where human blood serum samples were employed for real sample analysis.

## 2.7. Electroanalytical measurements

All electrochemical measurements were performed using 0.1 M PBS (pH=7.0) as the supporting electrolyte, which is degassed with nitrogen for 10 minutes to avoid the interference from the reduction of oxygen present in the aqueous electrolyte during the measurements. The cyclic voltammograms were obtained by scanning the potential from -0.3 V to +0.8 V vs. SCE at a fixed scan rate of 100 mV s<sup>-1</sup>. The current measurements were performed using DPV in a potential range between +0.0 V and +0.6 V and to record DPVs a step potential of 8 mV, a modulation amplitude of 50 mV and a scan rate of 16 mV s<sup>-1</sup> were employed. Electrochemical impedance spectroscopy (EIS) experiments were recorded at half-wave peak potential of the redox mixture consisting of 1 mM [Fe(CN)<sub>6</sub>]<sup>3-/4-</sup> solution along with 100 mM KCl as a supporting electrolyte using frequency ranging from 100 kHz to 0.1 Hz and 5 mV as the amplitude of alternating current.

## 2.8. Instrumentation

Electrochemical studies using voltammetric and electrochemical impedance spectroscopic (EIS) measurements were performed using Eco Chemie, Electrochemical workstation, model Autolab 302N using GPES software version 4.9 and frequency response analyzer (FRA), software version 2.0 respectively. A three electrode system employing gold disc electrode (BAS Inc.) as a working electrode, saturated calomel electrode (SCE) as a reference electrode and a spiral platinum (Pt) wire as a counter electrode were used in this work. All potentials referred in the text were against SCE. Toshniwal pH meter was used for measuring pH of the solutions. Surface morphologies of the prepared polymers were analyzed with a help of FESEM (Carl Zeiss, Supra 35 VP, Germany). FTIR spectra of these samples were recorded using Shimadzu model IR Affinity FTIR spectrophotometer.

### 3. Results and Discussion

#### 3.1. Selection of functional monomer for the preparation of MIP

A virtual library of 15 functional monomers is analyzed to select the most suitable functional monomer. The interaction energy values between EP and each of these functional monomers were calculated and presented in Table 1. The interaction energy of such pre-polymer complex is directly related to its stability.<sup>37</sup> From the computational studies, TAT is identified to be the most promising functional monomer capable of forming stronger interactions with the template, EP. This may be due to the formation of multiple interactions in well defined three dimensional preferences with the functional monomer, TAT.<sup>38</sup> This particular monomer is used further to prepare the molecularly imprinted polymer (MIP) using EP as a template.

#### 3.2. Characterization of EP imprinted polymer

Structure and morphology of EP imprinted MIP were characterized using FTIR and FESEM analyses. FTIR spectra were recorded for synthesized EP imprinted microspheres (MIP), before (B) and after (C) the extraction of EP along with the non-imprinted microspheres (NIP) prepared in absence of EP (A) and the corresponding spectra were shown in Figure 1. EP MIP before extraction (Fig. 1B) showed a broad band in the region  $2950 - 3490 \text{ cm}^{-1}$  due to the hydrogen bonding between  $-\text{NH}$  group of TAT and  $-\text{OH}$  group of EP. Shifting of the hydroxyl group of EP and  $-\text{NH}$  of TAT from  $3500$  to  $3490 \text{ cm}^{-1}$  and  $3350$  to  $2990 \text{ cm}^{-1}$  respectively were attributed to the formation of hydrogen bonding. This shift essentially arises due to the non-covalent interactions, i.e., hydrophobically driven hydrogen bonding between TAT and EP. On the other hand, non-imprinted polymers (Fig. 1A) do not show any such kind of shift in

peaks to lower region suggesting the absence of template, EP. Some common bands were observed for TAT, hemin and EGDMA viz.,  $1726\text{ cm}^{-1}$  corresponds to C=O stretching;  $1458\text{ cm}^{-1}$  attributed to  $-\text{CH}_2$  and  $-\text{CH}_3$  deformation and  $1161\text{ cm}^{-1}$  due to C–O vibration. It is interesting to notice that a broad band in the region  $2950 - 3300\text{ cm}^{-1}$  disappeared in the EP extracted MIP spectra (Fig. 1C), indicating a complete removal of EP.

Further FESEM analysis was carried out to investigate the structural and morphological changes occur in the resultant MIP and for comparison a similar study using NIP was also performed. Figure 2 shows the FESEM images of EP imprinted (A) and non-imprinted (B) polymers. FESEM image of MIP (Fig. 2A) clearly reveals the formation of uniformly sized, discrete and nearly monodispersed particles resembling microspheres, whereas the NIP (Fig. 2B) displays an irregular and highly agglomerated particles. This indicates the possible ordered cross linker reactions and imprinted effect of MIP on the resultant microspheres.

### 3.3. Electrochemical characterization of MIP coated Au electrodes

Electrochemical impedance spectroscopy (EIS) is used for investigating and analyzing the electron transfer characteristics of EP imprinted and non-imprinted polymers modified Au electrodes. Formation of semicircle in EIS is generally used for the determination of charge transfer resistance ( $R_{ct}$ ) value. Impedance spectra of various modified electrodes were recorded using  $0.1\text{ M KCl}$  containing  $5\text{ mmol L}^{-1} [\text{Fe}(\text{CN})_6]^{3-/4-}$  as a redox probe with a small excitation amplitude of  $5\text{ mV}$  peak to peak over the frequency range of  $100\text{ kHz}$  to  $100\text{ mHz}$  and the respective plots were shown in Figure 3. In order to determine the  $R_{ct}$  values the collected impedance data were best fitted to Randle's equivalent circuit. From these Nyquist plots it is evident that bare Au surface (Fig. 3a) exhibited a semi circle with higher  $R_{ct}$  of  $868\ \Omega$ ,

suggesting a relatively sluggish electrochemical performance of the redox probe on bare Au electrode.<sup>39</sup> Further  $R_{ct}$  values at Au electrode modified with NIP (Fig. 3b) and MIP before extraction of EP (Fig. 3c) remarkably decreased to 155  $\Omega$  and 198  $\Omega$  respectively. It is very interesting to notice that after the extraction of template, MIP coated Au electrode (Fig. 3d) showed a very less  $R_{ct}$  value of 57  $\Omega$ , indicating the formation of cavities due to removal of EP, which facilitate and enhance the electron transfer characteristics at the MIP modified electrode interface.<sup>40</sup> These results confirm the surface modification using MIP and NIP microspheres and EP–MIP modified Au electrode shows a facilitated electron transfer process along with a good electrical conductivity.

In order to confirm the changes in  $R_{ct}$  values are due to modified EP–MIP films, impedance studies were performed at various steps of chitosan and Nafion coated electrodes for EP–MIP system before and after extraction of EP using the same above mentioned electrolyte solution consisting of a redox probe along with a supporting electrolyte. Results obtained from these studies (supporting information; Fig. S3) clearly rule out the possibility of electrostatic attraction between chitosan and the redox probe along with the repulsive interaction between Nafion and the redox probe. These studies clearly indicate that the observed changes in  $R_{ct}$  values are mainly due to the process of imprinting and due to the removal of template, EP by extraction.

### 3.4. Electrochemical detection of EP using MIP modified Au electrodes

EP imprinted MIP modified Au electrodes were explored further for the possible application in electrochemical detection of EP. The mechanism associated with EP sensing relies mainly on the cascade reaction involving redox change of EP at molecularly imprinted

microspheres that act as a catalyst. This reaction involves the oxidation of EP to EP-quinone while the hemin unit present within MIP is reduced and further the oxidized form of hemin is regenerated by H<sub>2</sub>O<sub>2</sub>. The presence of H<sub>2</sub>O<sub>2</sub> in the electrolyte aids the conversion of reduced hemin to oxidized hemin and in-turn enhances the EP sensing process. Overall the proposed electrochemical biosensor has essentially two active sites namely MIP and hemin. It is interesting to note that both these active sites play a crucial role and break down EP for its electrochemical detection resulting in cascade reaction mechanism. The principle of EP detection is illustrated in Figure 4. Quantification of EP is determined by monitoring the electrochemical reduction of EP-quinone species on the electrode surface by the application of a suitable potential. The mechanism is similar to those proposed for the electrochemical determination of glucose and determination of phenolic compounds using biomimetic catalysts such as dopamine  $\beta$ -monooxygenase, peroxidase and tyrosinase enzymes.<sup>41</sup> This particular mechanism also explains the higher sensitivity of the proposed sensor arising from the signal amplification due to the cascade of redox reactions.<sup>42,43</sup>

EP oxidized product EP-quinone is electrochemically active and could be reduced at electrode surface to produce an amplified response.<sup>44</sup> Both cyclic voltammetry (CV) and DPV measurements were employed to evaluate the electrochemical activity of EP-MIP modified Au electrode towards EP detection. CV studies were carried out in 0.1 M PBS (pH=7.0) solution at a fixed potential sweep rate of 100 mV/s (supporting information; Fig. S4). Formation of redox peaks in CV is attributed to EP and EP-quinone redox couple and this correlates very well with the proposed cascade reaction mechanism for EP sensing where this redox couple plays a critical role. Interestingly, the change in redox current due to incremental addition of EP is very minimum; making it very difficult to distinguish. On contrary, differential pulse voltammetry

(DPV) assays exhibit significant changes in the reduction current due to elimination of double layer charging current associated with the modified electrodes and maximizes the signal to noise ratio. These experiments were performed by sweeping the potential between 0.0 V and 0.6 V by monitoring the redox reaction of EP and EP–quinone formation.<sup>45</sup> The comparative DPV responses of MIP and NIP coated Au disc electrodes obtained after subtraction of background current were displayed in Figure 5. The reduction current is significantly increased at MIP modified Au electrode (Fig. 5b) after the addition of  $10 \mu\text{mol L}^{-1}$  EP. On contrary NIP microspheres coated electrode (Fig. 5a) did not show any response in the absence and presence of EP, indicating the absence of active sites for EP detection. In contrast, MIP modified electrodes show peak formation at 380 mV due to the formation of EP–quinone species on adding EP, indicating the effect of cascade reactions essentially arising from the hemin unit present within the immobilized microspheres that could be oxidized by  $\text{H}_2\text{O}_2$  and re-reduced by the added analyte, EP. In order to prove that this sensing mechanism works only in presence of  $\text{H}_2\text{O}_2$ , a few other experiments were also carried out using CV studies. These CVs were recorded using EP–MIP coated Au electrodes in PBS solution with out  $\text{H}_2\text{O}_2$  and along with a fixed concentration of EP (supporting information; Fig. S4). The respective cyclic voltammograms show clearly that EP–MIP coated Au electrode shows a clear redox peak corresponding to EP and EP–quinone redox reaction only if  $\text{H}_2\text{O}_2$  is present. This cyclic reaction is particularly responsible for EP detection as illustrated in Figure 4.

### 3.5. Optimization of conditions

From electrochemical studies it is clear that EP–MIP modified Au electrode could be used for the detection of EP and it is necessary to optimize the conditions at which the proposed

electrochemical sensor works better and exhibits good sensor characteristics namely sensitivity, limit of detection, linear concentration range and stability etc. First of all the quantity of EP imprinted microspheres to be used for coating onto the working electrode for fabrication of the sensor is analyzed. Insufficient amount of active sites cannot provide suitable amplification of the analyte response. On the other hand, higher amount of MIP microspheres can lead to slow diffusion of analyte to the recognition sites and hence results in an inefficient communication between the binding sites and transduction.<sup>46</sup> Henceforth the optimization of various parameters and conditions is absolutely necessary for any sensor. The change in DPV peak current with respect to increase in reaction time was examined by coating 10, 20, 30 and 50  $\mu\text{g}$  of EP imprinted microspheres onto the working electrode (supporting information; Fig. S5A). It is identified that the sensors prepared with 10, 20 and 30  $\mu\text{g}$  of microspheres showed increase in peak current during the initial 20 minutes, while 50  $\mu\text{g}$  microspheres coated sensor exhibited decrease in reduction current till 20 minutes and a slight increase after 20 minutes (supporting information; Fig. S5A). The sensor prepared with 10  $\mu\text{g}$  of microspheres found to display a rapid increase and the higher reduction current, suggesting a suitable communication between the reaction product, EP-quinone and the electrode surface. Gradual decrease in analyte response with increase in quantity of microspheres may be attributed to the increase in resistance of the electrode surface that inhibits the transduction response. Hence, 10  $\mu\text{g}$  of microspheres with an incubation time of 20 minutes was considered as the optimal value.

Similarly, the dependence of sensor response on  $\text{H}_2\text{O}_2$  concentration in the range of 50 – 500  $\mu\text{mol L}^{-1}$  was studied (supporting information; Fig. S5B) since it plays a vital role in cascading the reaction of peroxidase enzymes, with higher concentrations inhibiting the catalysis.<sup>47</sup> It is noticed that at a fixed EP concentration of 10  $\mu\text{mol L}^{-1}$ , the variation in reduction

current increased with H<sub>2</sub>O<sub>2</sub> concentration and reached a maximum at 200 μmol L<sup>-1</sup> (supporting information; Fig. S5B). Hence this concentration was chosen for all the subsequent experiments.

Moreover, the influence of pH on the reduction peak current of EP–quinone was also investigated in the pH range of 2–10. As the pH of medium was gradually increased, the peak current reached its maximum value at pH 7.0 and at pH higher than 7.0, the reduction current was found to decrease (supporting information; Fig. S5C). This is due to the negative charge on the EP–quinone species that inhibits the reduction at higher pH values. So, the pH of detection medium was selected to be 7.0 and optimized.

### **3.6. Evaluation of electrochemical sensor characteristics for EP detection using DPV studies**

Finally, EP–MIP microspheres coated Au disc electrode fabricated under optimized conditions was used as a sensing platform to monitor the changes in reduction current values by following DPV assay, as shown in Figure 6. EP reduction current increases with systematic increasing concentration of EP suggesting an efficient electrocatalytic property of MIP microspheres due to the presence of specific cavities formed during the polymerization. The reaction product EP–quinone is reduced resulting in the formation of a peak and the response was explored via DPV (Fig. 6A). It is evident from the analysis that increasing concentration of EP results in increased reduction current, suggesting the potential applicability of MIP electrodes as a sensor matrix. To quantify, the change in reduction current at the peak value was plotted against the concentration of EP (Fig. 6B). It is observed that there are two linear ranges from  $5.0 \times 10^{-8} \text{ M} - 1.1 \times 10^{-6} \text{ M}$  and  $1.1 \times 10^{-6} \text{ M} - 40 \times 10^{-6} \text{ M}$  with the regression equations  $\Delta i (\mu\text{A})$

$= -0.4588 + 0.2222 [\text{EP}] \mu\text{mol L}^{-1}$  ( $R^2 = 0.9890$ ) and  $\Delta i (\mu\text{A}) = -0.7152 + 0.0066 [\text{EP}] \mu\text{mol L}^{-1}$  ( $R^2 = 0.9895$ ).

At concentrations above  $40 \mu\text{mol L}^{-1}$  the sensor exhibits saturation and follows Michaelis–Menten behaviour with a  $K_m$  value of  $18.23 \mu\text{mol L}^{-1}$ . The molecularly imprinted polymers as recognition elements behave similar to biosensors constructed with the natural enzymes and also possess advantages such as low cost, high stability and ease of preparation.<sup>48,49</sup> The detection limit and linear concentration range values were calculated according to the IUPAC recommendations and those values were found to be  $1.2 \times 10^{-8}$  M and  $5.0 \times 10^{-8}$  to  $40 \times 10^{-6}$  M respectively. Compared with other sensors described in the literature over the past decade for EP detection, the proposed sensor in this work displayed a significant improvement in detection limit and comparable linear concentration range as shown in Table 2.<sup>28,45,50–54</sup> Further to investigate the reproducibility and repeatability of the proposed electrochemical sensor, several experiments were performed in PBS (pH=7.0) solution containing  $200 \mu\text{mol L}^{-1}$   $\text{H}_2\text{O}_2$  with addition of  $10 \mu\text{mol L}^{-1}$  EP into the electrochemical cell and recording the change in reduction current ( $\Delta i$ ) as the sensor response to the target analyte. The EP–MIP electrode exhibited a relative standard deviation (RSD) value of 4.4% of reduction peak current for a series of five sensors prepared in the same manner. Similarly, there was no significant change in the response even after 25 measurements. The current response was observed to be retained 95% of its initial value after 20 days. These results clearly demonstrate very good stability and reproducibility of the imprinted sensors.

### 3.7. Selectivity of the EP Sensor

In order to evaluate the selectivity of synthesized MIP, three compounds which are structural analogues to EP viz., (-)-Isoproterenol hydrochloride (IP), dihydroxy naphthalene (DN), 3,4-dihydroxy-L-phenylamine (HPA) and two other compounds namely 3,4-dihydroxy hydrocinnamic acid (HCA) and L-ascorbic acid (LAA) with different structures but capable of forming quinone derivatives were considered in this study. DPV experiments were carried out by monitoring the change in reduction current for both MIP and NIP modified Au electrodes toward EP sensing in presence of these interferences at two different concentrations viz., 10  $\mu\text{M}$  and 20  $\mu\text{M}$  and the corresponding data were displayed in Figure 7. EP imprinted microspheres based sensor showed at least five times more current response for EP-quinone than non-imprinted microspheres based sensor. It is evident from these results that in case of interferences, there is no significant difference in the response exhibited by MIP and NIP microspheres modified electrodes, proving the specific selectivity towards EP for the synthesized MIP microspheres (Fig. 7). It is very interesting to notice that although IP nearly possess the same structure as EP, the response of the sensor is much lower than that for EP. This suggests the high selectivity of the sensor mainly arises due to the specific recognition sites, and not merely the cavities, which reflect the process of templating during the polymerization in terms of size, shape and arrangement of the functional groups.

### 3.8. Analytical applicability of proposed EP sensor

Analytical applicability of the proposed method was investigated for the determination of EP in human serum samples and injection solutions. EP hydrochloride injection samples (standard content of EP 1  $\text{mg mL}^{-1}$ ; 1 mL per injection) were purchased from a local pharmacy with proper approval and permission as mentioned above. Human blood serum samples were

obtained from a local pathology clinic with a proper permission as stated in the experimental section and it was stored under refrigeration. 50  $\mu\text{L}$  of serum samples were diluted with 9.5 mL of PBS (pH=7.0) solution to avoid the interferences arising from the serum matrix. Basically we varied the concentration of EP in these samples from 1  $\mu\text{M}$  to 10  $\mu\text{M}$  and analyzed the determination of EP using the proposed electrochemical sensor (supporting information; Table S1). The corresponding comparison values obtained from this EP sensor were shown in Table 3. These results clearly indicate the recovery percentages for both injection and human serum samples are in the range of 96–112% and RSD is between 1.75 and 5.48. These values demonstrate a highly promising analytical applicability of the proposed biomimetic sensor for electrochemical determination of EP in pharmaceutical and real samples analyses.

#### 4. Conclusions

Rational synthesis of a new sensory MIP material for electrochemical detection of EP is presented and EP imprinted microspheres are prepared by a precipitation polymerization method. Gold disc electrode is modified with microspheres of MIP for the electrochemical sensing of EP. Under optimized conditions, MIP modified Au electrodes exhibit a higher electrocatalytic activity, better sensitivity and selectivity towards EP detection in comparison to NIP modified electrode. This confirms the formation of shape specific and site selective cavities during polymerization for the target analyte molecule. Electrochemical interface properties of the bare and MIP/NIP modified electrodes are studied by using EIS. MIP modified electrode shows a less charge transfer resistance than NIP modified surface. The proposed method is applied for the determination of EP in human serum and pharmaceutical samples and the obtained results are

more than satisfactory. This work clearly demonstrates the biomimetic polymers (MIPs) as promising materials to be used as artificial receptors for the electrochemical sensing of EP.

### Supplementary Data

Supporting information consisting of more results and analysis (Figure S1 to Figure S5 and Table S1) is available for this article.

### Acknowledgements

Authors are thankful to Dr. S. Umadevi, UGC–Asst. Prof., Department of Industrial Chemistry, Alagappa University, Karaikudi for her technical guidance in synthesis of the functional monomer. V. G. acknowledges the funding from Council of Scientific and Industrial Research (CSIR), India through 12<sup>th</sup> five year plan network project namely Molecules to Materials to Devices (M2D) having a project number CSC 0134.

### References

1. Q. M. Xue, *Physiological and Pathological Chemistry of Nervous System*, Science Press, Beijing, 1978, pp. 102–129.
2. T. N. Deftereos, A. C. Calokerinos and C. E. Efstathiou, *Analyst*, 1993, **118**, 627–632.
3. G. Wulff, *Chem. Rev.*, 2003, **102**, 1–28.
4. E. Fischer, *Ber Dtsch. Chem. Ges.*, 1894, **27**, 2985–2993.
5. J. A. Garcia-Calzon and M. E. Diaz-Garcia, *Sens. Actuators B: Chem*, 2007, **123**, 1180–1194.
6. L. Chen, S. Xuab and J. Li, *Chem. Soc. Rev.*, 2011, **40**, 2922–2942.

7. Z. Zhang, J. Li, L. Fu, D. Liua and L. Chen, *J. Mat. Chem. A*, 2015, **3**, 7437–7444.
8. T. Alizadeh, M. R. Ganjali, M. Zare and P. Norouzi, *Electrochim. Acta*, 2010, **55**, 1568–1574.
9. M. S. Ureta-Zanartu, P. Bustos, C. Berrios, M. C. Diez, M. L. Mora and C. Gutierrez, *Electrochim. Acta*, 2002,**47**, 2399–2406.
10. K. K. Tadi and R. V. Motghare, *J. Mol. Model.*, 2013, **19**, 3385–3396.
11. C. F. Van Nostrum, *Drug Discov. Today*, 2005, **2**, 119–120.
12. D. Batra and K. J. Shea, *Curr. Opin. Chem.. Biol.*, 2003, **7**, 434–442.
13. Y. Dineiro, M. I. Menendez, M. C. Blanco-Lopez, M. J. Lobo-Castanon, A. J. M. Ordieres and P. Tunon-Blanco, *Anal. Chem*, 2005,., **77**, 6741–6746.
14. M. Azenha, P. Kathirvel, P. Nogueira and A. Fernando-Silva, *Biosens. Bioelectron.*, 2008, **23**, 1843–1849.
15. M. Khan, P. Wate and R. J. Krupadam, *J. Mol. Model.*, 2012, **18**, 1969–1981.
16. R. Liu, X. Li, Y. Li, P. Jin, W. Qin and J. Qi, *Biosens. Bioelectron.*, 2009, **25**, 629–634.
17. S. Riahi, M. R. Ganjali and A. B. Moghaddam, *Spectrochim. Acta A*, 2008, **71**,1390–1396.
18. M. A. Fotopoulou and P. C. Loannou, *Anal. Chim. Acta*, 2002, **462**, 179–185.
19. Y. Y. Su, J. Wang and G. N. Chen, *Talanta*, 2005, **65**, 531–536.
20. P. Canizares and L. D. Castro, *Anal. Chim. Acta*, 1995, **317**, 335–341.
21. M. Zhu, X. Huang, J. Li and S. Hansi, *Anal. Chim. Acta*, 1997, **357**, 261–267.
22. L. Y. Zhang, Q. Sanfu, Z. L. Wang and J. L. Cheng, *J. Chromatogr. B*, 2003, **792**, 381–385.
23. J. X. Du, L. H. Shen and J. R. Lu, *Anal. Chim. Acta*, 2003, **489**, 183–189.
24. R. N. Goyal, V. K. Gupta and S. Chatterjee, *Biosens. Bioelectron.*, 2009, **24**, 1649–1654.

25. J. Hu, Y. Yu, J. C. Brooks, L. A. Godwin, S. Somasundaram, F. Torabinejad, J. Kim, C. Shannon and C. J. Easley, *J. Am. Chem. Soc.*, 2014, **136**, 8467–8474.
26. J. Hu, T. Wang, J. Kim, C. Shannon and C. J. Easley, *J. Am. Chem. Soc.*, 2012, **134**, 7066–7072.
27. X. Jiang and X. Lin, *Analyst*, 2005, **130**, 391–396.
28. H. S. Wang, D. Q. Huang and R. M. Liu, *J. Electroanal. Chem.*, 2004, **570**, 83–90.
29. Y. X. Sun, S. F. Wang and X. H. Zhang, *Sens. Actuators B: Chem*, 2006, **113**, 156–161.
30. B. B. Prasad, M. Rashmi, P. T. Mahavir and S. P. Sindhu, *Sens. Actuators B: Chem*, 2010, **146**, 321–330.
31. G. Diaz-Diaz, M. C. Blanco-López, M. J. Lobo-Castanon, A. J. Miranda-Ordieres and P. Tunon-Blanco, *Electroanal.*, 2011, **23**, 201–208.
32. R. S. W. Jesus, R. L. Phabyanno, R. T. T. Cesar, F. H. Nelci and T. K. Lauro, *Anal. Chim. Acta*, 2009, **631**, 170–176.
33. B. Liu, H. T. Lian, J. F. Yin and X. Y. Sun, *Electrochim. Acta*, 2012, **75**, 108–114.
34. J. Wang, M. Musameh and Y. H. Lin, *J. Am. Chem. Soc.*, 2003, **125**, 2408–2409.
35. K. K. Tadi and R. V. Motghare, *J. Chem. Sci.*, 2013, **125**, 413–418.
36. S. F. Boys and F. Bernardi, *Mol. Phys.* 1970, **19**, 553–566.
37. S. Piletsky, K. Karim, E. V. Piletska, C. J., Day, K. W. Freebairn, C. Legge and A. P. F. Turner, *Analyst*, 2001, **126**, 1826–1830.
38. R. Maffezzoni and M. Zanda, *Tetrahedron Lett.*, 2008, **49**, 5129–5132.
39. F. Li, J. Li, Y. Feng, L. Yang and Z. Du, *Sens. Actuators B: Chem.*, 2011, **157**, 110–114.
40. K. Koteswara Reddy and K. Vengatajalabathy Gobi, *Sens. Actuators B: Chem.*, 2013, **183**, 356–363.

41. F. S Damos, M. D. P. T. Sotomayor, L. T. Kubota, S. M. C. N. Tanaka and A. A Tanaka, *Analyst*, 2003, **128**, 255–259.
42. F. Lisdat, U. Wollenberger, A. Makower, H. Hortnagl, D. Pfeiffer and F. W. Scheller, *Biosens. Bioelectron.*, 1997, **12**, 1199–1211.
43. C. Nistor, J. Emnéus, L. Gorton and A. Ciucu, *Anal. Chim. Acta*, 1999, **387**, 309–326.
44. Z. Hui-Min, Z. Xian-Liang, H. Ru-Tai, I. Nan-Qiang and L. De-Pei, *Talanta*, 2002, **56**, 1081–1088.
45. W. Liang, B. Junyue, H. Pengfei, W. Hongjing, Z. Liying and Z. Yuqing, *Electrochem. Commun.*, 2006, **8**, 1035–1040.
46. C. Xie, H. Li, S. Li, J. Wu and Z. Zhu, *Anal. Chem.*, 2010, **82**, 241–249.
47. S. S. Razola, B. L. Ruiz, N. M. Diez, Jr. Mark and H. B. Kauffmann, *Biosens. Bioelectron.*, 2002, **17**, 921–928.
48. R. Z. Ouyang, H. P. Lei, H. X. Ju and Y. D. Xue, *Adv. Funct. Mater.*, 2007, **17**, 3223–3230.
49. J. Ma, L. H. Yuan, M. J. Ding, S. Wang, F. Ren, J. Zhang, S. H. Du, F. Li and X. M. Zhou, *Biosens. Bioelectron.*, 2011, **26**, 2791–2795.
50. S. Saeed, G. Masoumeh and K. A. Mohammad, *Sens. Actuators B: Chem*, 2009, **137**, 669–675.
51. B. B. Prasad, A. Prasad, T. Mahavir Prasad and M. Rashmi, *Biosens. Bioelectron.*, 2013, **45**, 114–122.
52. H. Chun-Wei and Y. Ming-Chang, *Sens. Actuators B: Chem*, 2008, **134**, 680–686.
53. F. Cui and X. Zhang, *J. Electroanal. Chem.*, 2012, **669**, 35–41.
54. H. Zhou, G. Xu, A. Zhu, Z. Zhao, C. C. Ren, L. Nie and X. Kan, *RSC Advances*, 2012, **2**, 7803–7808.

**Table-1:**

Interaction energy values obtained for the formation of pre-polymer complexes between EP and various functional monomers employed for the computational study.

S. No.	Functional monomer	Interaction energy <sup>a</sup> $\Delta E$ (k cal mol <sup>-1</sup> )
1.	EP – 2,4,6-Trisacrylamido-1,3,5-triazine	-43.9507
2.	EP – p-Vinyl benzoic acid	-37.9957
3.	EP – Uraconic acid	-37.3744
4.	EP – <i>trans</i> -3-Pyridyl acrylic acid	-36.4834
5.	EP – Itaconic acid	-35.1531
6.	EP – 2-(Trifluoromethyl) acrylic acid	-31.6578
7.	EP – Acrylamide	-30.7479
8.	EP – Methacrylic acid	-30.5848
9.	EP – Acrylic acid	-30.3965
10.	EP – 4(5) Vinylimidazole	-28.5768
11.	EP – 4-Vinyl pyridine	-27.9242
12.	EP – N,N-methylene bisacrylamide	-26.5248
13.	EP – Acrylonitrile	-26.0855
14.	EP – Allylamine	-25.0062
15.	EP – Acrylamido 2-(methyl) 1-propane sulphonic acid	2.324

<sup>a</sup> BSSE corrected interaction energies

**Table–2:**

Comparison of the various electrochemical methods reported for EP determination.

S.No.	Method	Electroanalytical technique used	Linearity range (M)	Detection limit (M)	Reference
1.	SAM <sup>a</sup> on gold electrode	Square wave adsorptive stripping voltammetry	$5.0 \times 10^{-7} - 1.0$ $\times 10^{-5}$ and $1.0 \times 10^{-5} - 6.0$ $\times 10^{-4}$	$1.0 \times 10^{-8}$	28
2.	SAM <sup>a</sup> on gold nanoparticles	Cyclic voltammetry	$1.0 \times 10^{-7} - 3.2$ $\times 10^{-8}$ and $1.0 \times 10^{-5} - 2.0$ $\times 10^{-4}$	$6.0 \times 10^{-8}$	45
3.	Ionic liquids/carbon nanotubes based carbon paste electrode	Differential pulse voltammetry	$3 \times 10^{-7} - 450 \times$ $10^{-6}$	$9.0 \times 10^{-8}$	49
4.	MIP in sol–gel on ITO <sup>b</sup> electrode	Amperometry	$1.0 \times 10^{-4} - 1.0$ $\times 10^{-3}$	--	50
5.	Carbon paste electrode/iron pthalocyanin	Differential pulse voltammetry	$1.0 \times 10^{-4} - 1.0$ $\times 10^{-3}$	$5 \times 10^{-6}$	51
6.	Gr/Au NPs/GCE <sup>c</sup>	Cyclic voltammetry	$5.0 \times 10^{-8} - 8.0$ $\times 10^{-6}$	$7.0 \times 10^{-9}$	52

7.	Electropolymerized MIP	Amperometry	$3 \times 10^{-7} - 1.0 \times 10^{-3}$	$9.0 \times 10^{-8}$	53
8.	MIP based sensor	Differential pulse adsorptive stripping voltammetry	$4.9 \times 10^{-10} - 3.2 \times 10^{-8}$	$1.1 \times 10^{-10}$	54
9.	Hemin modified MIP	Differential pulse voltammetry	$5.0 \times 10^{-8} - 1.1 \times 10^{-6}$ and $1.1 \times 10^{-6}$ to $40 \times 10^{-6}$	$1.2 \times 10^{-8}$	Present work

---

<sup>a</sup> SAM – Self Assembled Monolayer

<sup>b</sup> Indium tin oxide

<sup>c</sup> Graphene/gold nanoparticles/glassy carbon electrode

**Table-3:**

Recovery studies of EP sensing in human blood serum and injection samples.

Samples	Added ( $\mu\text{mol L}^{-1}$ )	Found ( $\mu\text{mol L}^{-1}$ )	Recovery (%, n=3)
	--	ND	--
Serum Sample	1.48	1.67	112.8 ( $\pm$ 3.46)
	2.91	3.22	110.6 ( $\pm$ 2.25)
	4.41	4.36	98.86 ( $\pm$ 2.45)
Injection sample	1.00	0.96	96 ( $\pm$ 5.48)
	3.46	3.65	105.5 ( $\pm$ 4.35)
	5.88	5.75	97.78 ( $\pm$ 1.75)

These results are expressed as mean values and the  $\pm$  RSD values are based on three replicate measurements.

**Figure captions:**

1. FTIR spectra of EP imprinted microspheres before and after extraction (B and C) along with the non-imprinted microspheres (A).
2. FESEM images of EP imprinted (A) and non-imprinted microspheres (B).
3. EIS of bare Au disc electrode (a), NIP (b) and MIP microspheres modified Au electrodes before (c) and after extraction (d) of EP in  $5 \text{ mmol L}^{-1} [\text{Fe}(\text{CN})_6]^{3-/4-}$  solution containing  $0.1 \text{ M}$  KCl as a supporting electrolyte. Inset: Equivalent circuit used for fitting the impedance data.
4. Schematic representation of the principle associated with the electrochemical detection of EP.
5. Baseline corrected DPV responses of (a) NIP and (b) EP–MIP modified Au disc electrodes in  $0.1 \text{ mol L}^{-1}$  PBS (pH=7.0) containing  $200 \text{ }\mu\text{mol L}^{-1}$   $\text{H}_2\text{O}_2$  and  $10 \text{ }\mu\text{mol L}^{-1}$  EP.
6. (A) DPV curves recorded in  $0.1 \text{ mol L}^{-1}$  PBS (pH=7.0) containing  $200 \text{ }\mu\text{mol L}^{-1}$   $\text{H}_2\text{O}_2$  at the MIP modified Au electrode for different EP concentrations: (a) blank (0 M), (b)  $5.00 \times 10^{-8}$  M, (c)  $4.03 \times 10^{-7}$  M, (d)  $7.98 \times 10^{-7}$  M, (e)  $1.13 \times 10^{-6}$  M, (f)  $5.84 \times 10^{-6}$  M, (g)  $10.07 \times 10^{-6}$  M, (h)  $13.94 \times 10^{-6}$  M, (i)  $20.75 \times 10^{-6}$  M, (j)  $26.54 \times 10^{-6}$  M, (k)  $30.15 \times 10^{-6}$  M, (l)  $35.93 \times 10^{-6}$  M and (m)  $40 \times 10^{-6}$  M respectively. (B) A plot of variation in reduction current vs. EP concentration. Inset: Similar plot shown at lower concentrations of EP.
7. Variation of reduction current at MIP and NIP microspheres modified electrodes towards EP detection and other potential interferents each added at  $10 \text{ }\mu\text{mol L}^{-1}$  and  $20 \text{ }\mu\text{mol L}^{-1}$  concentrations. Supporting electrolyte:  $0.1 \text{ mol L}^{-1}$  PBS (pH=7.0) containing  $200 \text{ }\mu\text{mol L}^{-1}$   $\text{H}_2\text{O}_2$ .

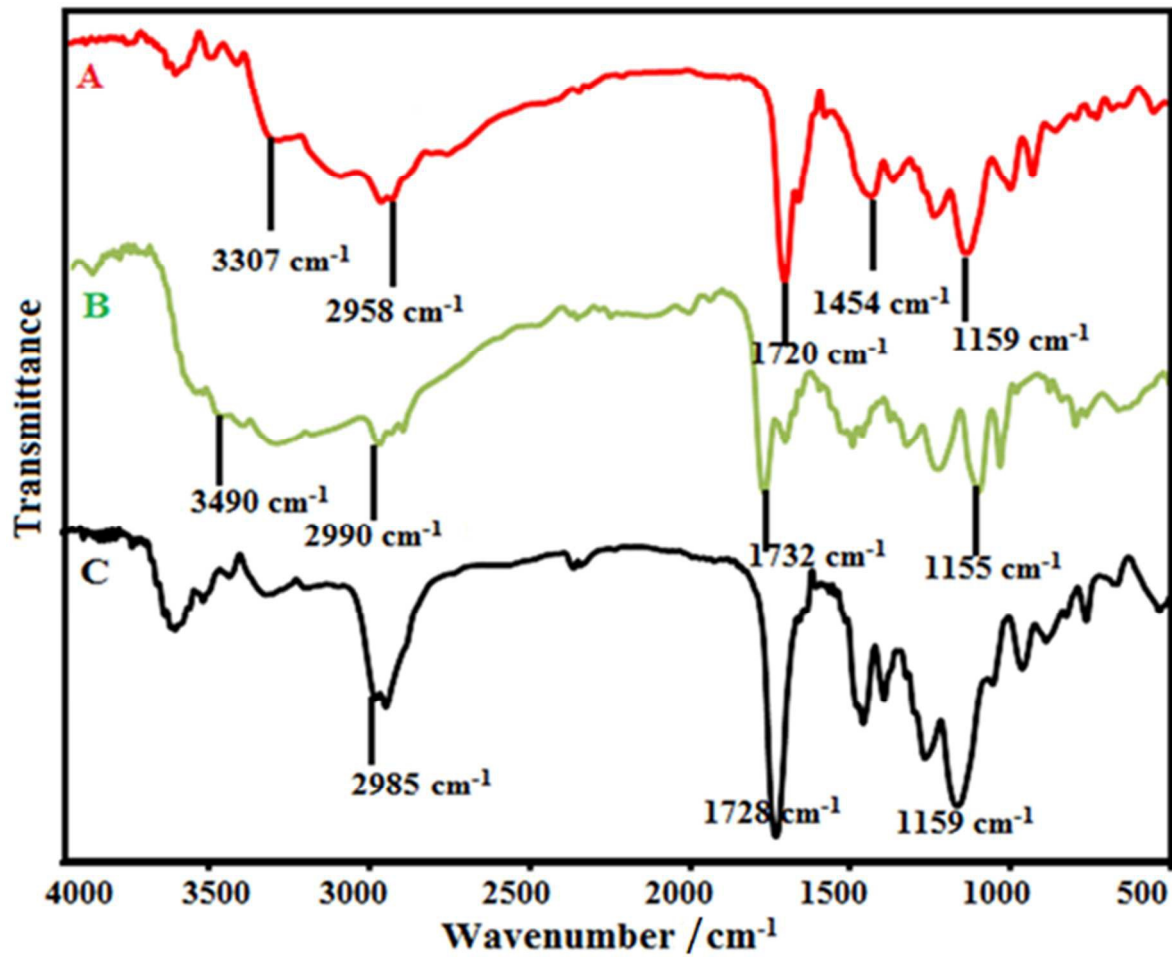


Figure 1

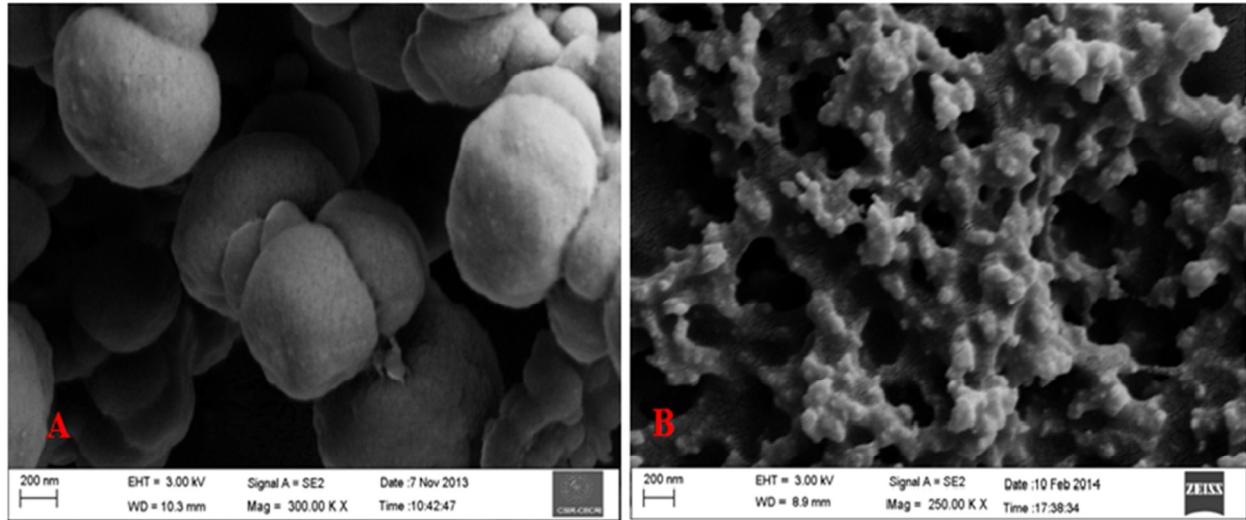


Figure 2

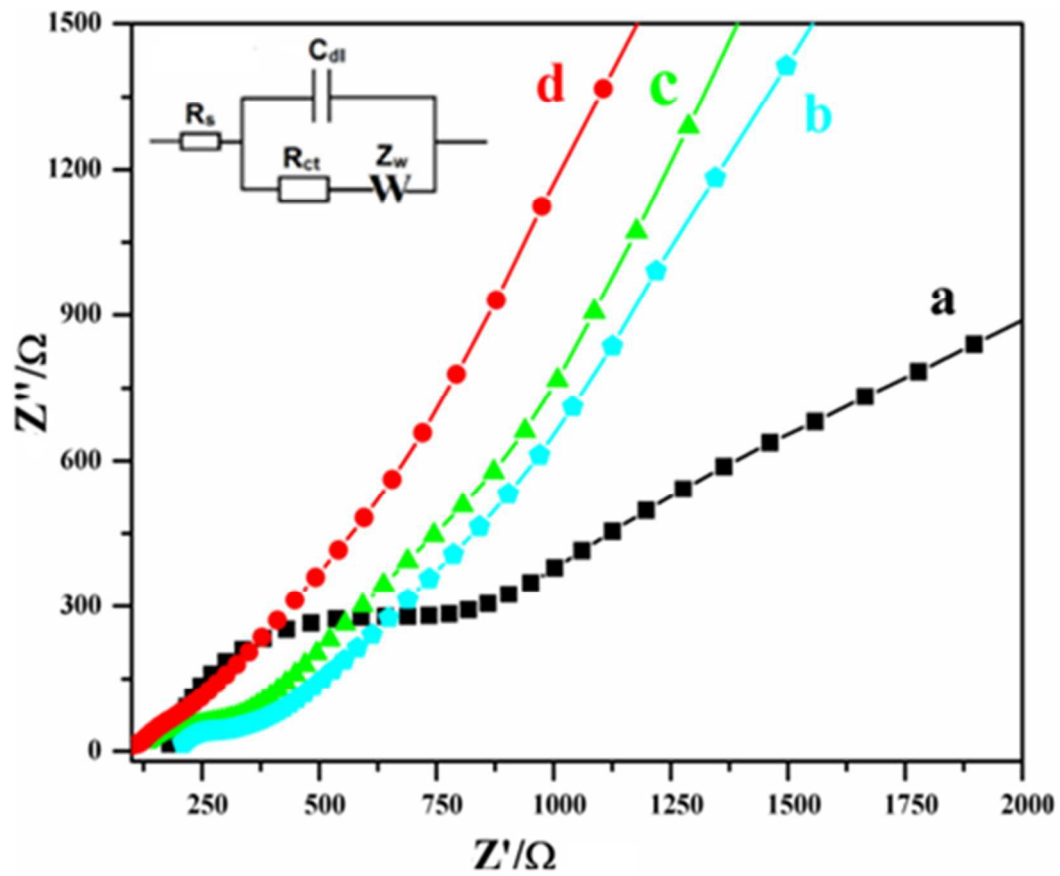


Figure 3

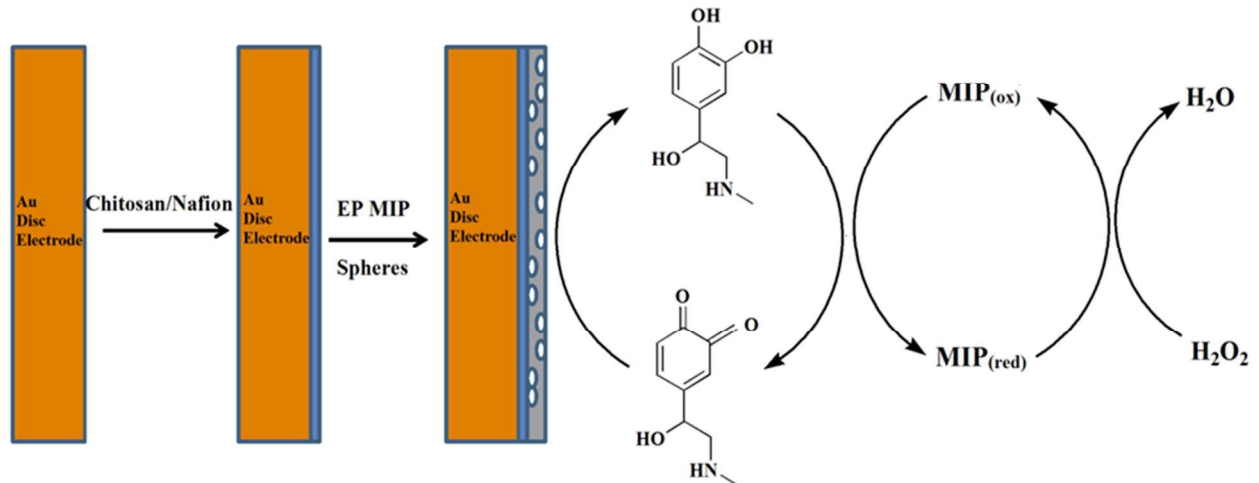


Figure 4

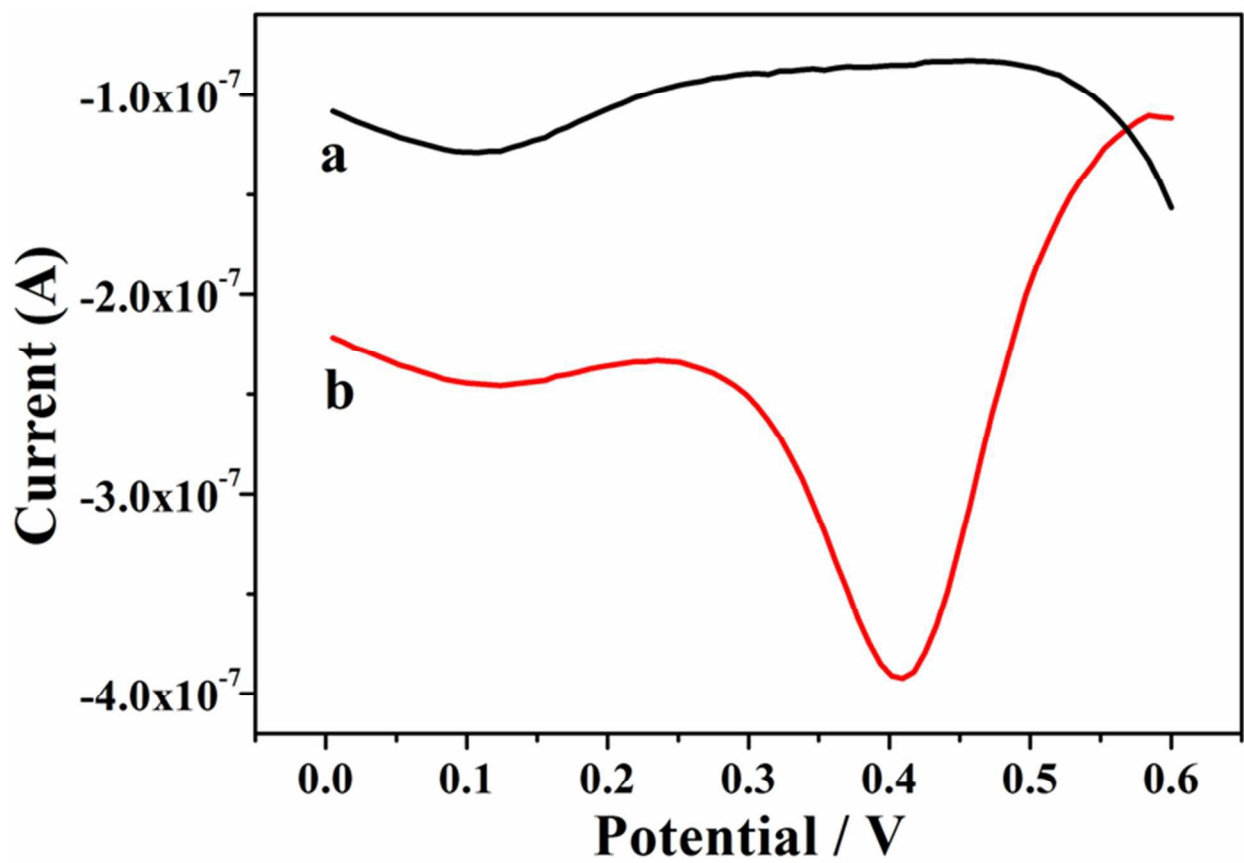


Figure 5

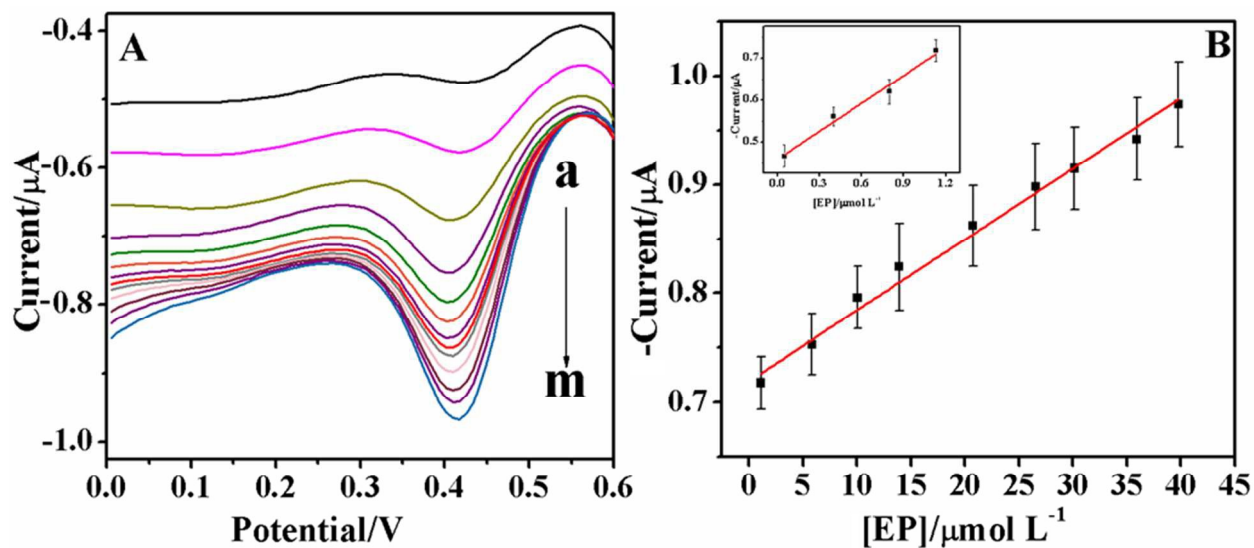


Figure 6

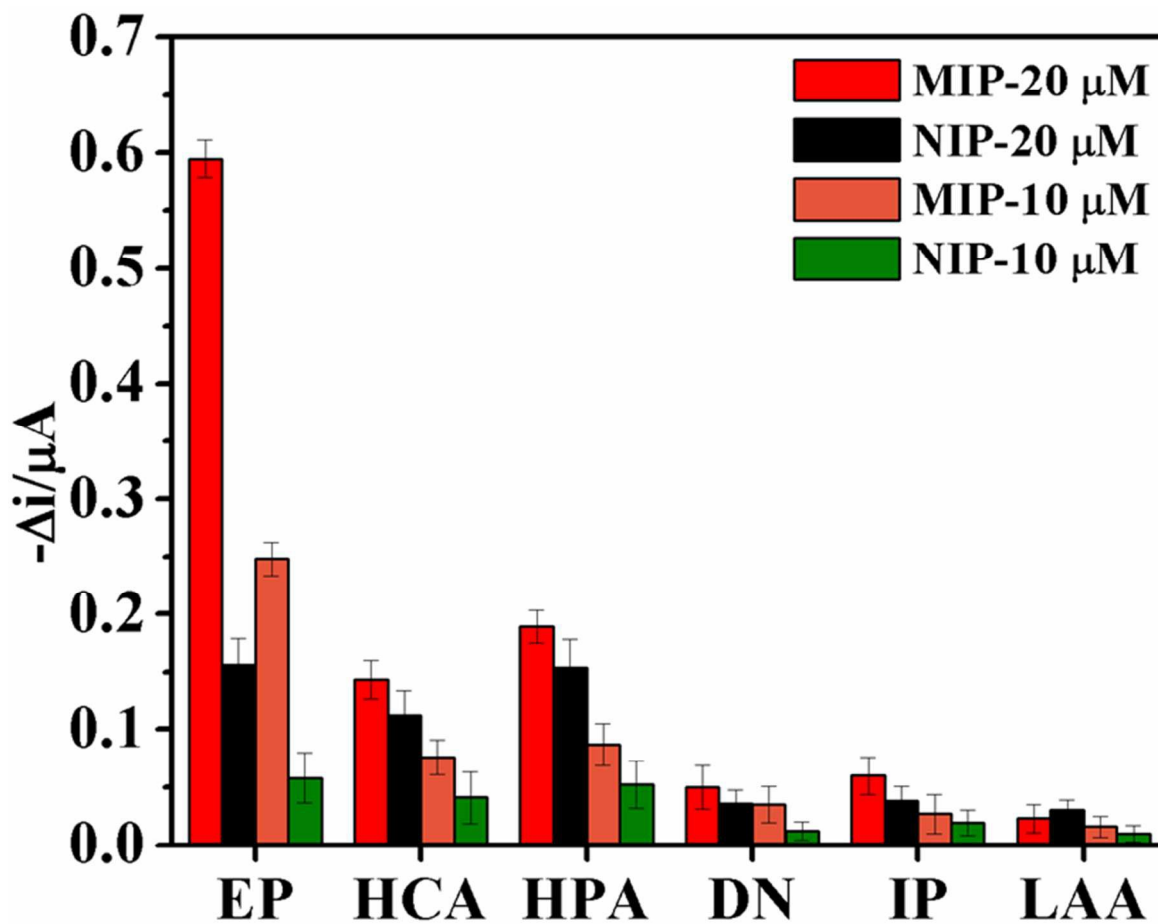


Figure 7